Efficient second-harmonic generation in nonlinear plasmonic waveguide

F. F. Lu, T. Li,* X. P. Hu, Q. Q. Cheng, S. N. Zhu, and Y. Y. Zhu

National Laboratory of Solid State Microstructures, College of Engineering and Applied Sciences, College of Physics, Nanjing University, Nanjing 210093, China

**Corresponding author: taoli@nju.edu.cn*

Received May 5, 2011; revised July 11, 2011; accepted July 30, 2011; posted August 1, 2011 (Doc. ID 147128); published August 23, 2011

We theoretically studied a nonlinear optical process in a hybrid plasmonic waveguide composed of a nonlinear dielectric waveguide and a metal film with a separation of a thin air gap. Owing to the hybridization effect of guided mode and surface plasmon polariton mode, this particular waveguide is able to confine the optical-field in a deep subwavelength scale together with low propagation loss. Based on this, efficient second-harmonic generations (SHG) were revealed at the fundamental wavelength of $\lambda = 1.55\,\mu$m with good field confinement. The SHG efficiency, as well as the coupling coefficient and mode area, were analyzed and discussed in detail with respect to the structural parameters.

OCIS codes: 240.6680, 190.4410, 230.7370, 230.7405.

Surface plasmon polariton (SPP), as a promising candidate that merges electrons and photons, provides possible approaches to confine the optical-field in the subwavelength scale, and therefore suggests potential applications in future nanophotonic integrations. Many fundamental components of plasmonic circuits, including directional couplers, Mach–Zehnder interferometers and ring resonators, have been successfully realized to manipulate optical signals in the nanoscale [1–3]. However, a full implement of nanophotonic integration reasonably requires the incorporation of nonlinear optics for signal process (e.g., optical switches [4]). Then, nonlinear effects in plasmonic systems are getting to attract increasing attention for tunable photonic manipulations [5–7].

To date, most of these proposed structures are designed in planar with only one-dimensional (1D) field confinement, making them impractical for applications in plasmonic integration. A major reason is that further confinement in planar dimension will inevitably increase the propagating loss of the SPP wave and dramatically lower down the nonlinear conversion efficiency. In fact, this problem has been widely analyzed in passive plasmonic waveguides of various types [8,9]. A well-defined configuration so-called dielectric-loaded waveguide was proved to have advantages in optimizing the subwavelength confinement and long propagation distance [9]. A more exciting structural development was made by Zhang *et al.* by introducing a low-index medium as a small gap between the high-index dielectric nanowire and metal surface [10], with which a deep subwavelength plasmonic laser was achieved [11].

In this Letter, we propose a similar structure as in [10], containing a nonlinear dielectric waveguide, to realize an efficient nonlinear optical process with two-dimensional (2D) confinement in subwavelength scale. Specifically, we investigate the second-harmonic generation (SHG) in this structure with the aid of quasi-phase-matching (QPM) technique [12]. It is found that, utilizing this structure, we are able to realize efficient SHG within a short propagation distance, which would be of great importance in future nanophotonic modulations. To make an in-depth recognition of the SHG process in this hybrid waveguide, the influence of the structural parameters is analyzed in detail.

Figure 1(a) shows the schematic of the nonlinear hybrid waveguide. The structure is composed of a rectangular $LiNbO_3$ (LN) nonlinear waveguide and a silver film, separated by a thin air gap. The *c*-axis of LN is orientated along the *z*-direction and is periodically poled with the domain wall perpendicular to the *x*-direction. Since E_z is the key component getting involved in the nonlinear process in such a configuration, we simulated the field distributions for the fundamental frequency (FF) (1550 nm) and the second-harmonic (SH) (775 nm) using COMSOL 3.5, as shown in Figs. 1(b) and 1(c), respectively. For the FF

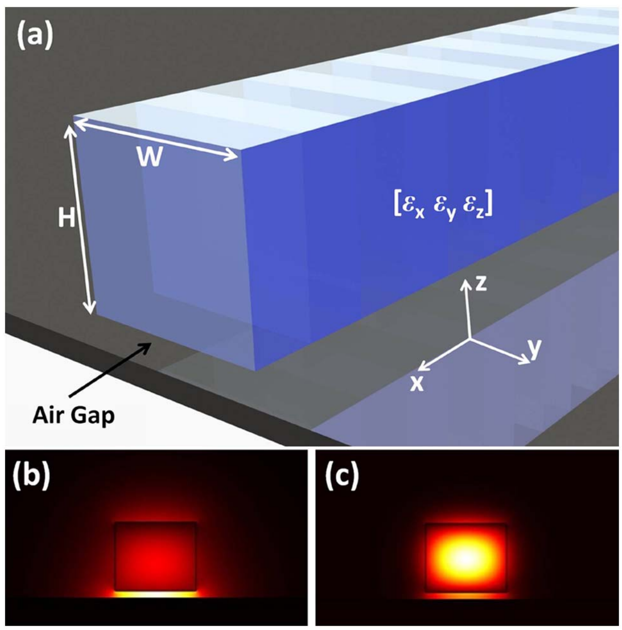

Fig. 1. (Color online) (a) Schematic of the nonlinear hybrid plasmonic waveguide. Here, metal is defined as silver and nonlinear dielectric is periodically poled $LiNbO_3$. Structural parameters are: $w = h = 500$ nm, gap $= 50$ nm. $\varepsilon_m = -126 + 3.4i$ (silver) for FF and $\varepsilon_m = -30.77 + 0.42i$ for SH, $[\varepsilon_x, \varepsilon_y, \varepsilon_z] = [4.89, 4.89, 4.57]$ ($LiNbO_3$) for FF, and [5.10, 5.10, 4.74] [14] for SH. Mode profile of E_z for (b) FF and (c) SH.

wave, due to the strong coupling of the evanescent fields of the SPP and the guided mode of LN waveguide, an SPP-like hybrid mode comes into being with the majority energy concentrated inside the air gap [10,13]. This mode successfully reduces the absorption loss while maintaining a very small mode area. The normalized mode area [10] (NMA, mode area divided by diffraction-limited area in free space) of FF is about 0.2, far below the diffraction limit in a vacuum. As for the SH wave, the coupling between the metal and the crystal becomes weaker due to its smaller wavelength, which results in a waveguide-like hybrid mode with more field concentrated inside the LN part [10,13]. This mode even has lower loss than the FF one since the field penetrated inside the metal part is further decreased. One point should be stressed here is that both the SPP-like and waveguide-like hybrid modes have much smaller losses than the pure SPP one.

To more clearly illustrate the property of the mode-overlap between the FF and SH, we plot the mode profiles correspondingly in Fig. 2(a). The hybridization features of mode profiles analog to [10] are clearly manifested, showing considerable mode-overlap inside the LN part, though one is SPP-like and the other is waveguide-like. Figure 2(b) shows the intensity evolutions of FF and SH by numerically solving the coupled wave equations [5,6]. The incident power of FF is 1 W, and the power intensity is estimated to be about $400\ \mathrm{MW/cm^2}$ [2]. According to the hybrid mode dispersion, the effective indices of FF and SH are $1.54 + 3.9 \times 10^{-4}i$ and $1.97 + 1.23 \times 10^{-5}i$, respectively. To compensate the wavevector mismatch $\Delta\beta = \beta_{\mathrm{SH}} - 2\beta_{\mathrm{FF}}$, the poling period of the LN nonlinear waveguide is calculated to be $1.81\ \mu$m, according to the reciprocal vector of $G = 2\pi/\Lambda = \Delta\beta$. From Fig. 2(b), we can see that the SH reaches its maximum at the propagation distance of about 1 mm, where the conversion efficiency is about 1.3%. Although the local-field enhancement of SPP-like FF does not contribute a lot in the frequency conversion process (because the enhancement effect occurs inside the air gap instead of in the nonlinear LN for FF), the conversion efficiency still gets greatly improved compared to previous reports [5–7] due to the low absorption.

In the following, we will get to detailed analyses of the influences of structural parameters on the SHG effect. In Fig. 3, the propagation length, coupling coefficient (only taking the overlap integral of the field of FF and SH into account), SHG efficiency, normalized mode area of FF, and the position when SH gets its maximum (defined as peak position) versus the gap thickness are plotted. During the calculation, the poling periods of LN vary correspondingly to satisfy the QPM condition for all cases and the incident FF power was fixed to be 1 W. When the air gap thickness increases, the field inside the LN part for SH will increase correspondingly due to the weakened coupling between the waveguide and SPP modes, while the FF field will concentrate more into the air gap. These opposite evolutions of FF and SH field distributions make the field overlap changing little, resulting in a small range of the coupling coefficient [only 2.0–2.4, as shown in Fig. 3(b)]. However, the propagation length of both FF and SH increase monotonically due to less loss [see Fig. 3(a)]. Since more energy of FF can be transferred to SH with much lower absorption, the conversion efficiency gets improved when the gap becomes larger.

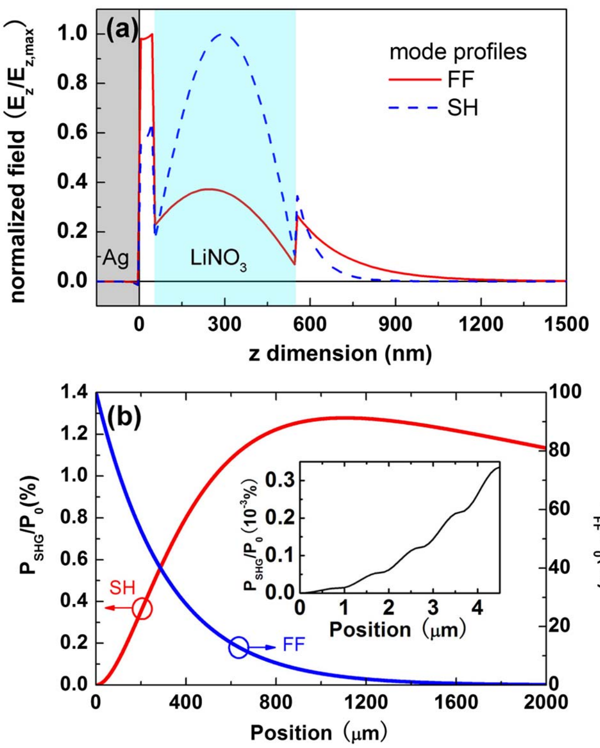

Fig. 2. (Color online) (a) Mode profiles of FF and SH in the cross-section (in z-dimension) of this particular hybrid waveguide. (b) Intensity evolutions of FF (blue) and SH (red) in the propagation. The inset shows the spatial evolution of SH in several periods at the very beginning.

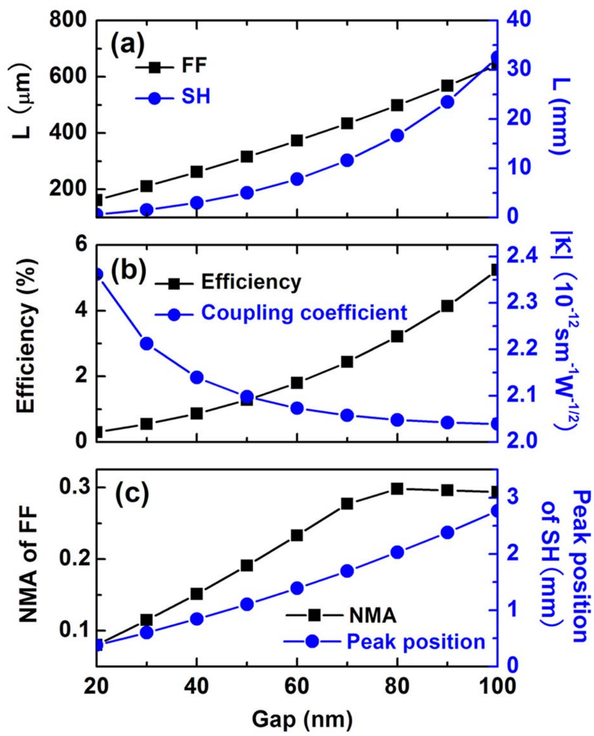

Fig. 3. (Color online) (a) Propagation length (L), (b) SHG efficiency and coupling coefficient ($|\kappa|$), (c) normalized mode area (NMA) of FF and peak position of SH as functions of the gap thickness.

Despite the SHG efficiency, it is necessary to stress that the mode area is another important factor to evaluate capability of this waveguide, which can be extremely small for the thin gap case (NMA ~ 0.08 of FF for 20 nm gap) and increases with the gap thickness, as shown in Fig. 3(c). When the gap reaches a considerably large value, the NMA tends to be unchanged because it is mainly determined by the pure SPP mode since the coupling is weak enough. In addition, we should notice that the peak position of SH also increases monotonously with the gap thickness, which means the maximum efficiency will be achieved in a farther distance if a larger gap is adopted, though it has a higher efficiency. Therefore, the proper choice of gap thickness in this SHG process is subject to trade-off between efficiency, mode area, and conversion rate (related to the peak position) as it is adopted in specific applications.

Besides, the influences of the height and width of the LN waveguide on the conversion efficiency and coupling coefficient are also analyzed as the results show in Fig. 4. Since the optical-field tends to concentrate in materials with a larger refractive index, increasing the size of the LN waveguide can reduce the field inside the silver film and lower the absorption in the metal, which will surely improve the conversion efficiency. In fact, the height of the LN waveguide plays a more important role in dominating the conversion efficiency compared with the width. The increase of the waveguide height effectively reduces the proportion of fields that penetrate into the air above and, thus, improves the mode-overlap and coupling coefficient. On the other hand, though the increase of waveguide width may attract more fields inside the LN part, it also undesirably reduces the power density. Consequently, the coupling coefficient increases at first and then drops slowly with widths ranging from 300 nm to 600 nm [see Fig. 4(b)].

To see the advantages of our proposed nonlinear plasmonic structure more clearly, we also explore the quasi-phase-matched SHG in a simple dielectric-loaded waveguide without gap (gap $= 0$, $w = h = 500\,\mathrm{nm}$, incident power $= 1\,\mathrm{W}$). Both the FF and SH are SPP mode in this case, and the field enhancement near to the metal surface greatly improves the field overlap between FF and SH. The coupling coefficient is about $4.36 \times 10^{-12}\,\mathrm{s \cdot m^{-1} \cdot W^{-1/2}}$, twice as much as that of the structure discussed above. However, the calculated SHG efficiency is only about 0.024%, much lower than this gap-employed waveguide. Although a large coupling coefficient in the no-gap waveguide means a higher conversion rate at the beginning that is beneficial to the SHG process, the high absorption loss of the SPP modes damages this advantage and the efficiency is surpassed by that of the gap-employed structure after only about $30 \sim 40\,\mu\mathrm{m}$ propagation.

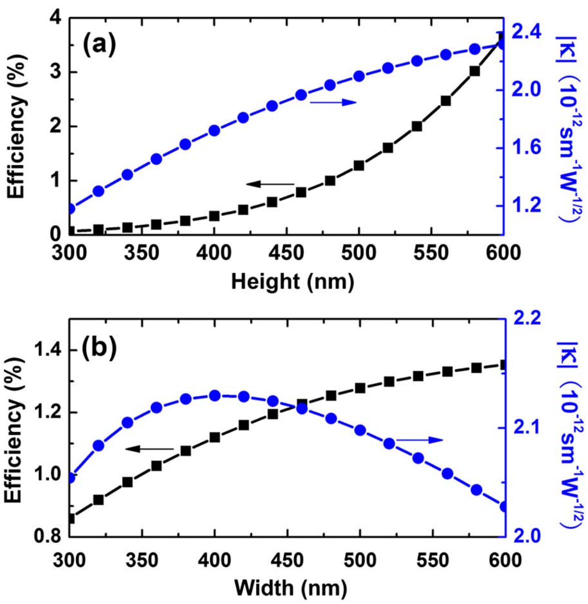

Fig. 4. (Color online) SHG efficiency and coupling coefficient versus (a) height and (b) width of the rectangular $LiNbO_3$ waveguide.

In conclusion, we theoretically proposed a nonlinear plasmonic waveguide with hybrid modes capable of good field confinement and low propagation loss, in which efficient SHGs were achieved from a SPP-like FF to a waveguide-like SH. In this waveguide, the air gap plays a dual role in confining the optical-field and reducing the mode loss, which improves the conversion efficiency with small mode area. Moreover, the influences of structural parameters on several important aspects of the SHG process were analyzed in detail, which considerably provides implications to optimize this nonlinear plasmonic waveguide for a particular purpose in plasmonic circuits or other manipulation of optical signals.

This work is supported by State Key Program for Basic Research of China (Nos. 2010CB630703, 2009CB930501), the National Natural Science Foundation of China (NSFC) (Nos. 10974090, 60 990 320, and 11 021 403).

References

1. Z. Chen, T. Holmgaard, S. I. Bozhevolnyi, A. V. Krasavin, A. V. Zayats, L. Markey, and A. Dereux, Opt. Lett. **34**, 310 (2009).
2. M. Pu, N. Yao, C. Hu, X. Xin, Z. Zhao, C. Wang, and X. Luo, Opt. Express **18**, 21030 (2010).
3. T. Holmgaard, Z. Chen, S. I. Bozhevolnyi, L. Markey, and A. Dereux, Opt. Express **17**, 2968 (2009).
4. Y. L. Lee, B. -A. Yu, T. J. Eom, W. Shin, C. Jung, Y. -C. Noh, J. Lee, and D. -K. Ko, Opt. Express **14**, 2776 (2006).
5. Z. J. Wu, X. K. Hu, Z. Y. Yu, W. Hu, F. Xu, and Y. Q. Lu, Phys. Rev. B **82**, 155107 (2010).
6. A. R. Davoyan, I. V. Shadrivov, and Y. S. Kivshar, Opt. Express **17**, 20063 (2009).
7. F. F. Lu, T. Li, J. Xu, Z. D. Xie, L. Li, S. N. Zhu, and Y. Y. Zhu, Opt. Express **19**, 2858 (2011).
8. S. I. Bozhevolnyi, Opt. Express **14**, 9467 (2006).
9. T. Holmgaard and S. I. Bozhevolnyi, Phys. Rev. B **75**, 245405 (2007).
10. R. F. Oulton, V. J. Sorger, D. F. P. Pile, D. A. Genov, and X. Zhang, Nat. Photonics **2**, 496 (2008).
11. R. F. Oulton, V. J. Sorger, T. Zentgraf, R. M. Ma, C. Gladden, L. Dai, G. Bartal, and X. Zhang, Nature **461**, 629 (2009).
12. Y. Q. Lu, Y. Y. Zhu, Y. F. Chen, S. N. Zhu, N. B. Ming, and Y. J. Feng, Science **284**, 1822 (1999).
13. L. Zhu, IEEE Photon. Technol. Lett. **22**, 535 (2010).
14. G. J. Edwards and M. Lawrence, Opt. Quantum Electron. **16**, 373 (1984).